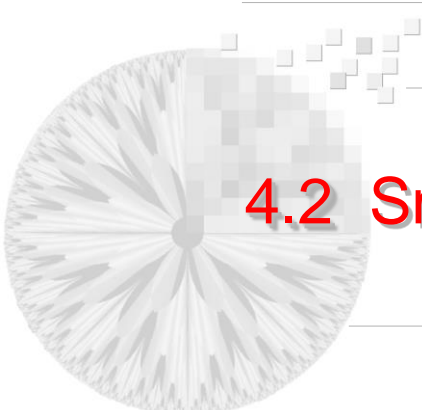


Chapter 4

Image Enhancement in the Frequency Domain

- 4.1 Fundamentals Related to Fourier Transform
- 4.2 Smoothing Using Frequency-Domain Filters
- 4.3 Sharpening Using Frequency-Domain Filters
- 4.4 Implementation**



4.2 Smoothing Using Frequency-Domain Filters

$$G(u, v) = H(u, v)F(u, v)$$

-- filter transfer function

4.2.1 Ideal Lowpass Filters (ILPF)

4.2.2 Butterworth Lowpass Filters (BLPF)

4.2.3 Gaussian Lowpass Filters (GLPF)

4.2.1 Ideal Lowpass Filter (ILPF)

$$H(u, v) = \begin{cases} 1 & \text{if } D(u, v) \leq D_0 \\ 0 & \text{if } D(u, v) > D_0 \end{cases}$$

$$D(u, v) = [(u - M/2)^2 + (v - N/2)^2]^{1/2}$$

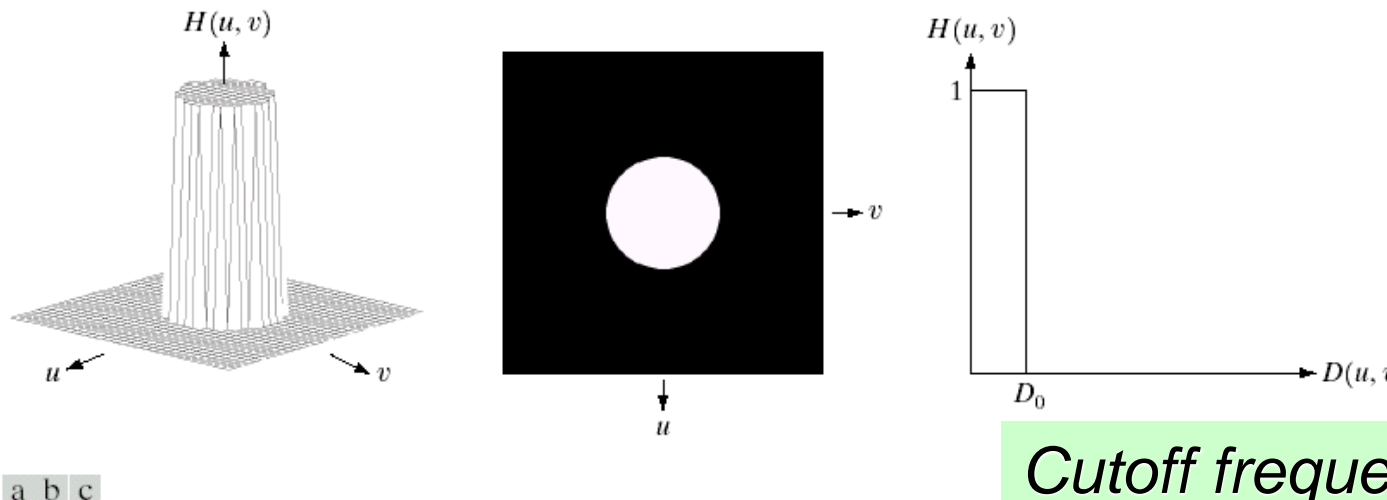
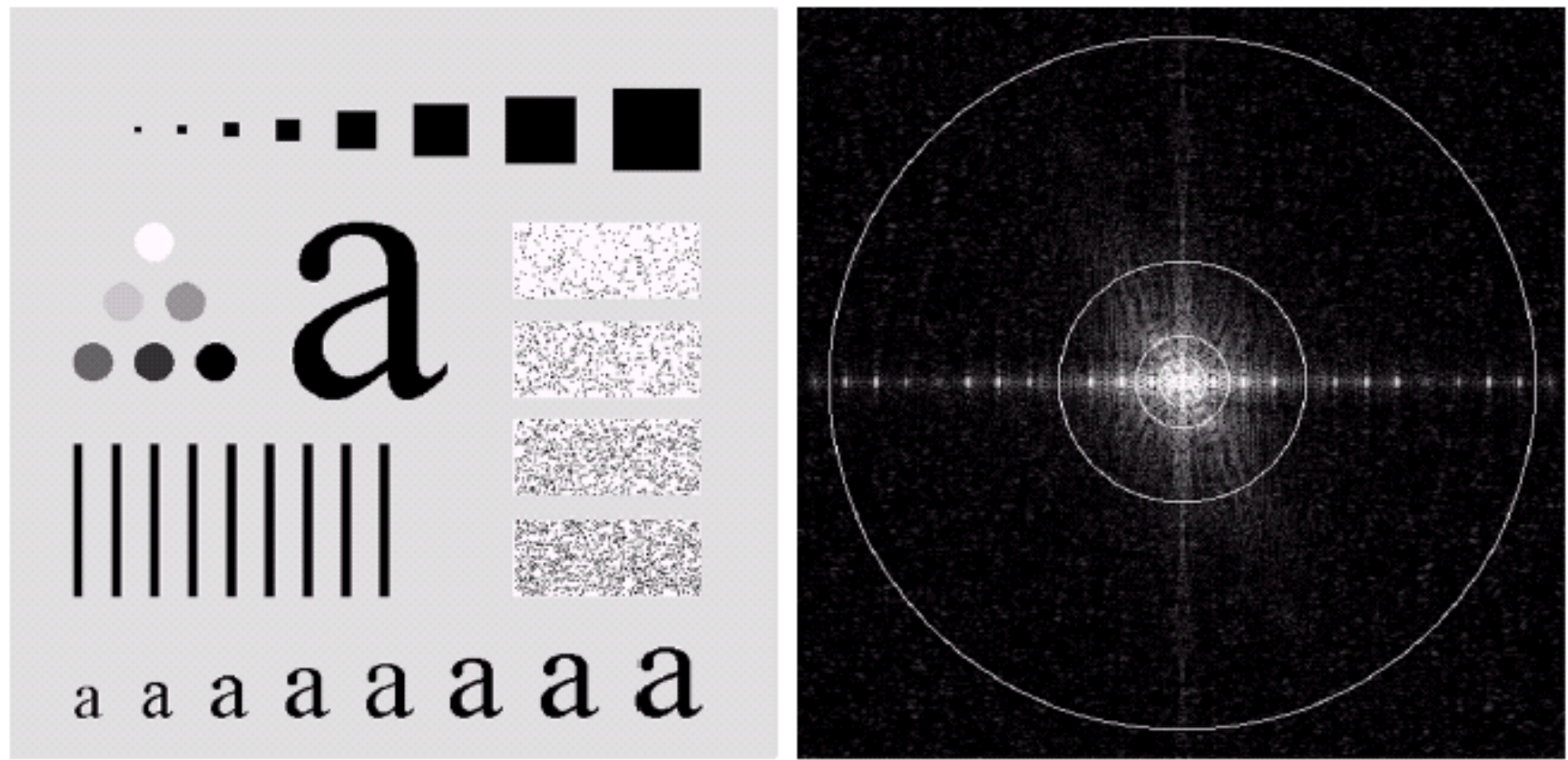


FIGURE 4.10 (a) Perspective plot of an ideal lowpass filter transfer function. (b) Filter displayed as an image. (c) Filter radial cross section.

Cutoff frequency loci



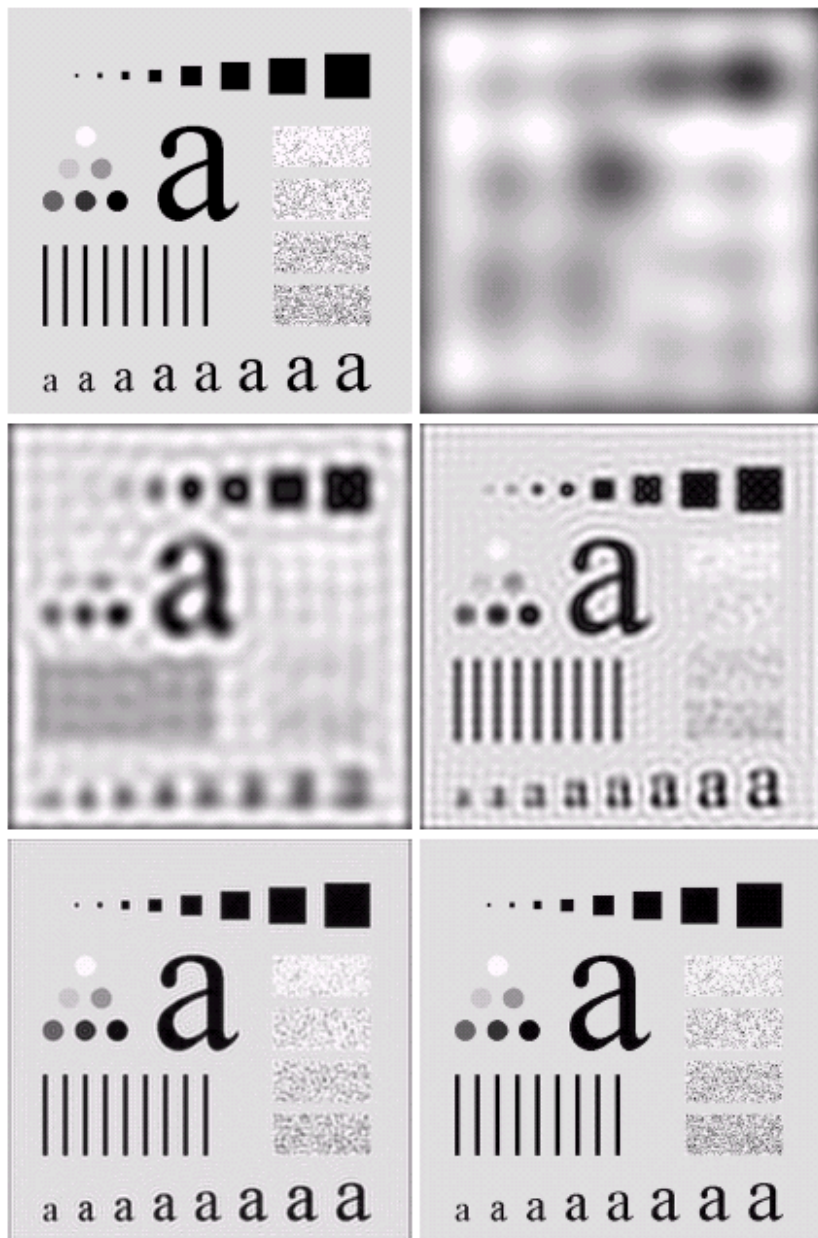
a b

FIGURE 4.11 (a) An image of size 500×500 pixels and (b) its Fourier spectrum. The superimposed circles have radii values of 5, 15, 30, 80, and 230, which enclose 92.0, 94.6, 96.4, 98.0, and 99.5% of the image power, respectively.



LPF: Blurring

Ringing effect!

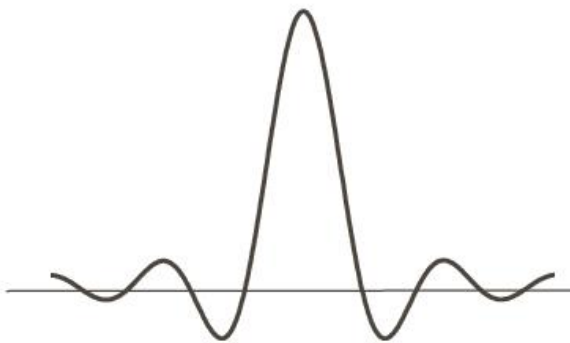
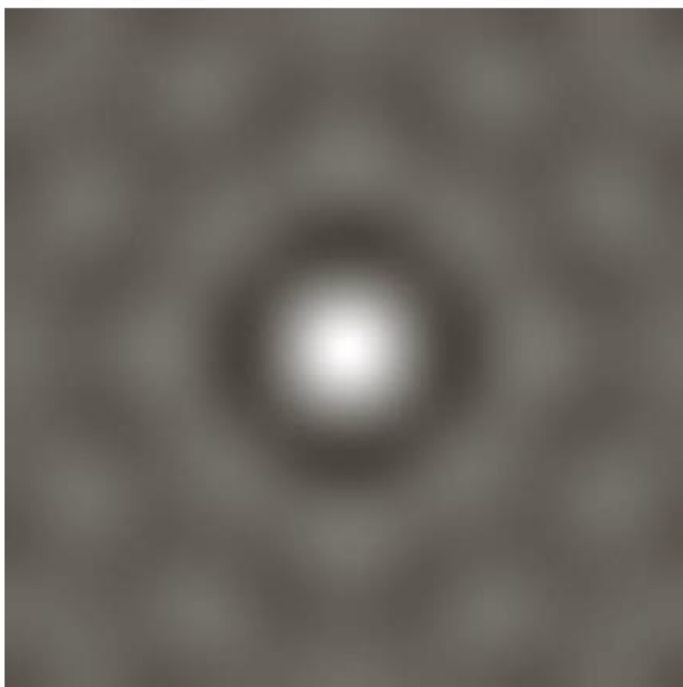


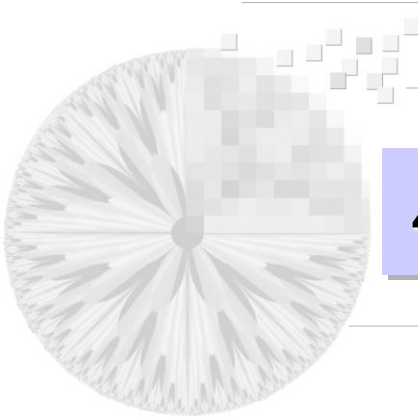
a b
c d
e f

FIGURE 4.12 (a) Original image. (b)–(f) Results of ideal lowpass filtering with cutoff frequencies set at radii values of 5, 15, 30, 80, and 230, as shown in Fig. 4.11(b). The power removed by these filters was 8, 5.4, 3.6, 2, and 0.5% of the total, respectively.

a b

FIGURE 4.43
(a) Representation in the spatial domain of an ILPF of radius 5 and size 1000×1000 .
(b) Intensity profile of a horizontal line passing through the center of the image.





4.2.2 Butterworth Lowpass Filters (BLPF)

$$H(u, v) = \frac{1}{1 + [D(u, v)/D_0]^{2n}}$$

n : filter order

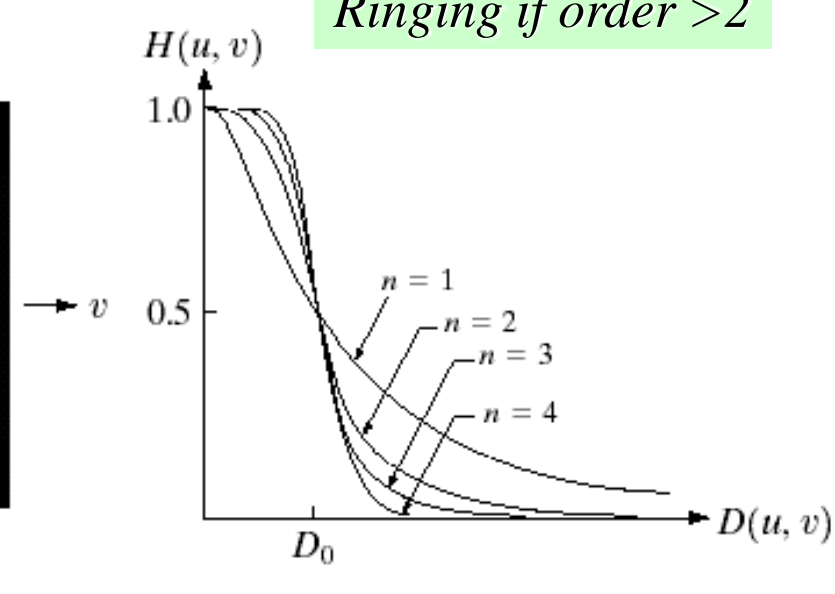
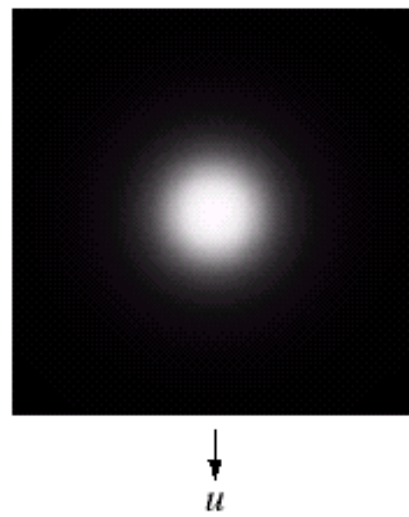
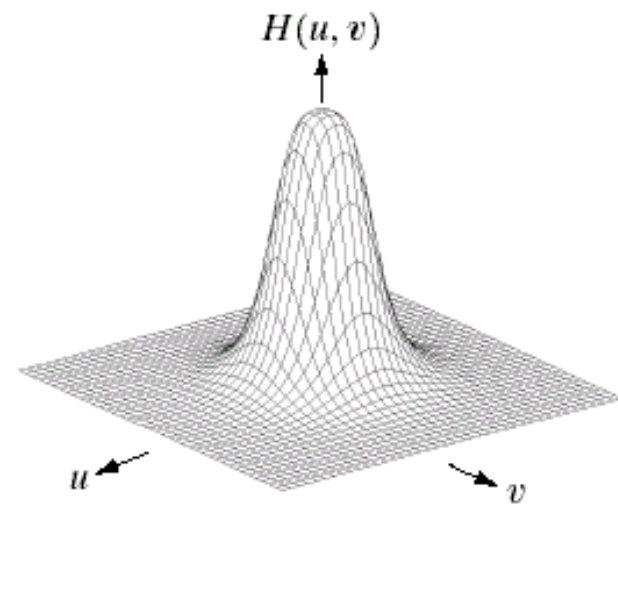
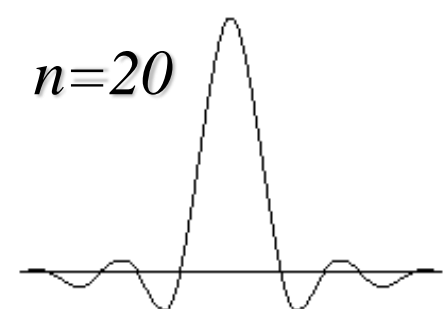
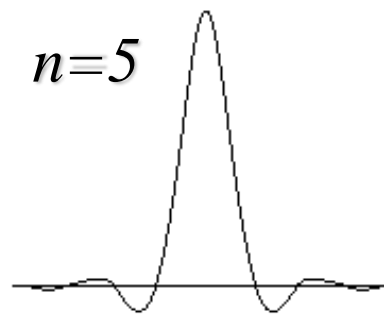
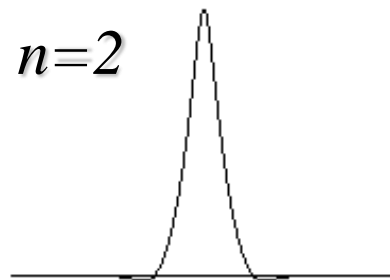
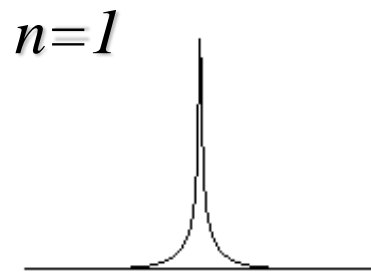
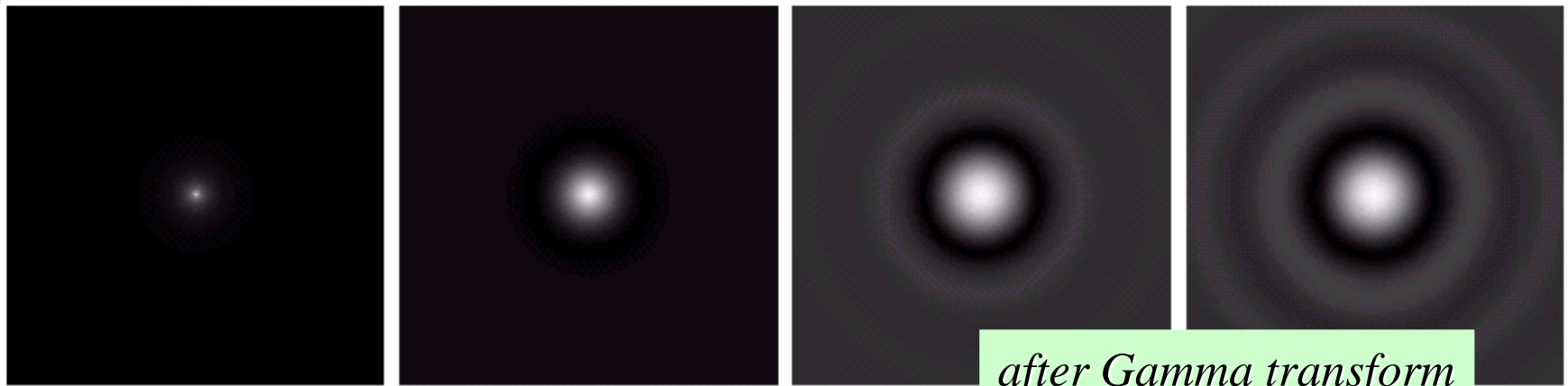
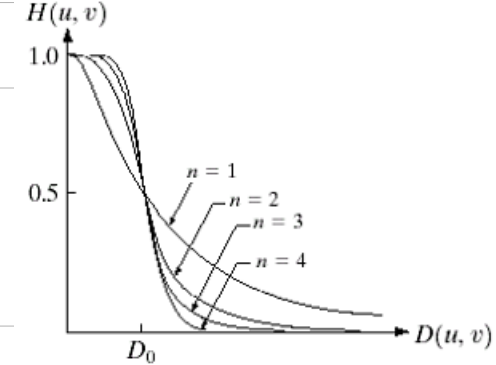


FIGURE 4.14 (a) Perspective plot of a Butterworth lowpass filter transfer function. (b) Filter displayed as an image. (c) Filter radial cross sections of orders 1 through 4.

Ringing of BLPF of different orders

$$D_0 = 5$$

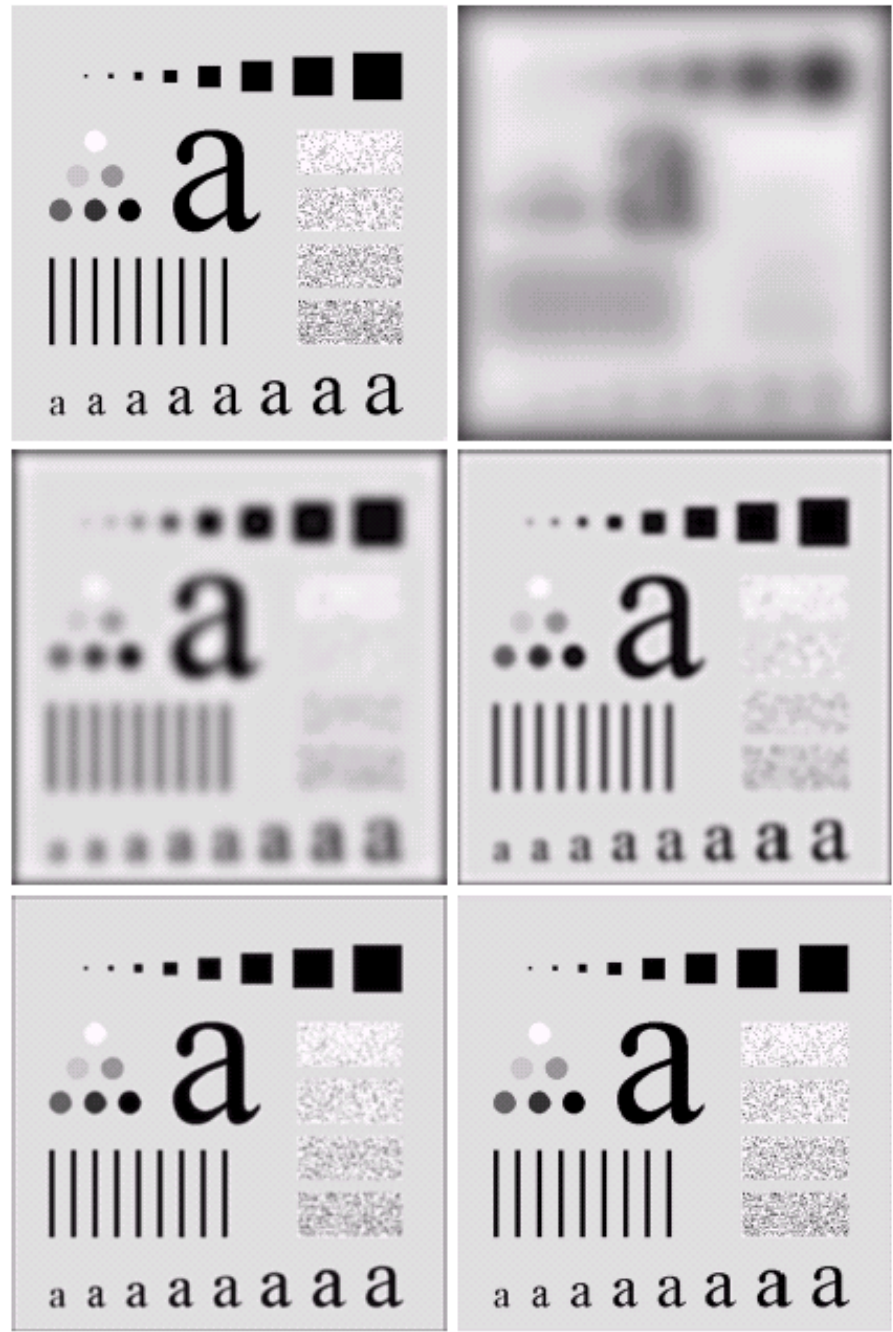


a b c d

FIGURE 4.16 (a)–(d) Spatial representation of BLPFs of order 1, 2, 5, and 20, and corresponding gray-level profiles through the center of the filters (all filters have a cutoff frequency of 5). Note that ringing increases as a function of filter order.



Order = 2



a
b
c
d
e

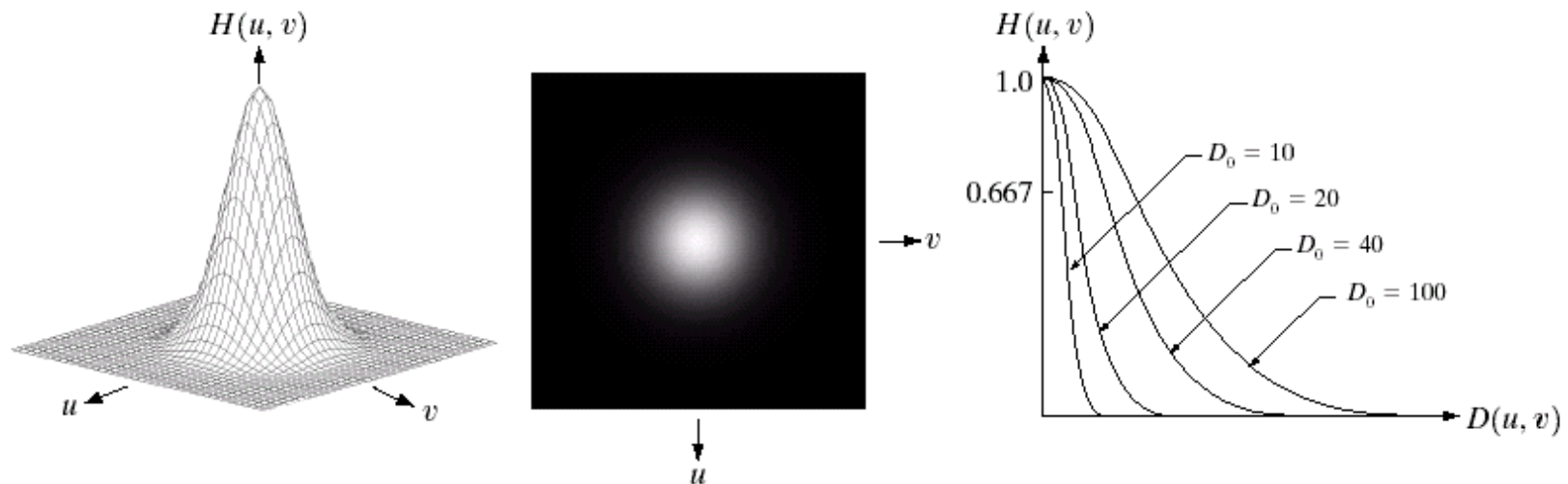
FIGURE 4.15 (a) Original image. (b)-(f) Results of filtering with BLPFs of order 2, with cutoff frequencies at radii of 5, 15, 30, 80, and 230, as shown in Fig. 4.11(b). Compare with Fig. 4.12.



4.2.3 Gaussian Lowpass Filters (GLPF)

$$H(u, v) = e^{-D^2(u, v)/2\sigma^2}$$

$$H(u, v) = e^{-D^2(u, v)/2D_0^2}$$



a b c

FIGURE 4.17 (a) Perspective plot of a GLPF transfer function. (b) Filter displayed as an image. (c) Filter radial cross sections for various values of D_0 .



No ringing!

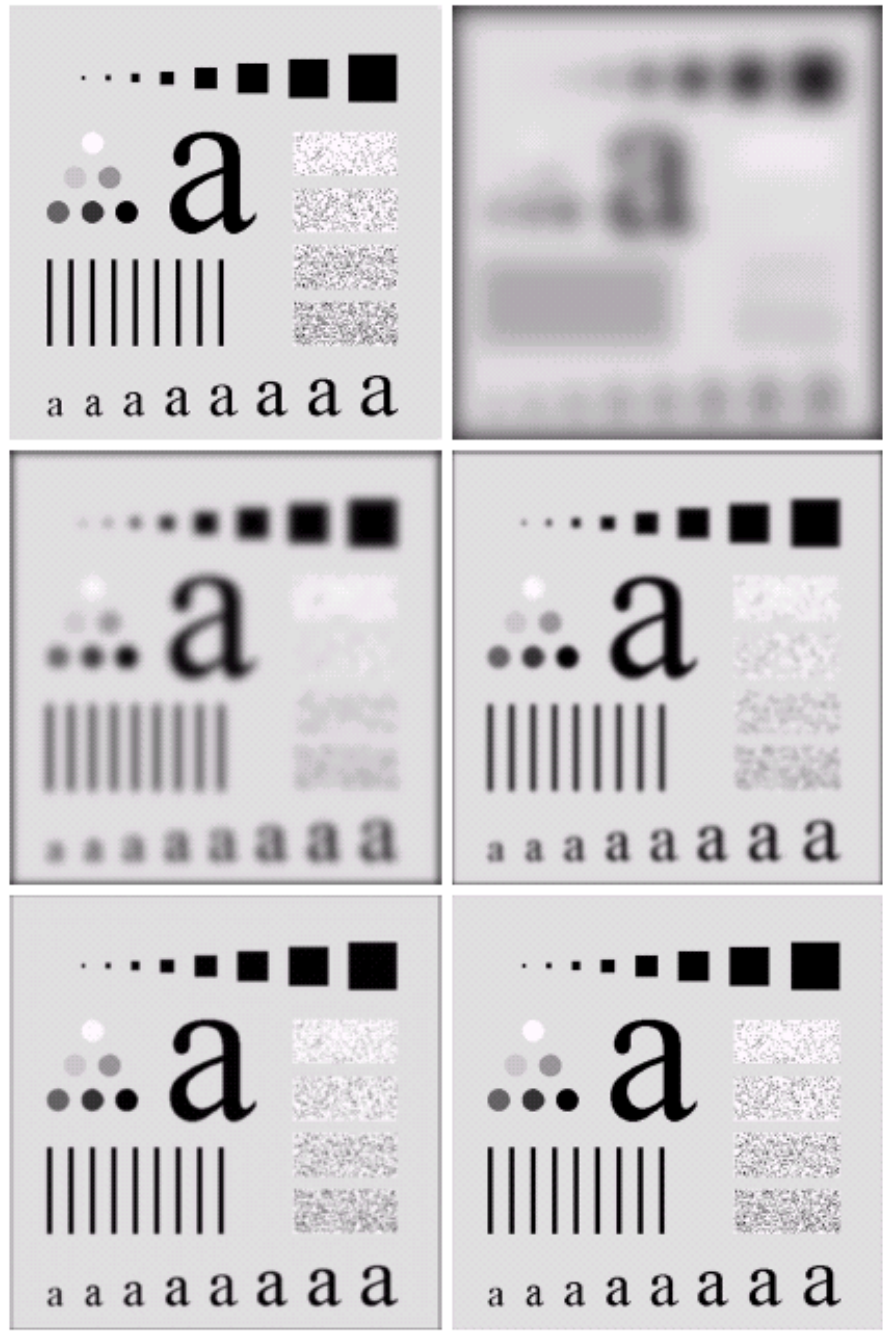
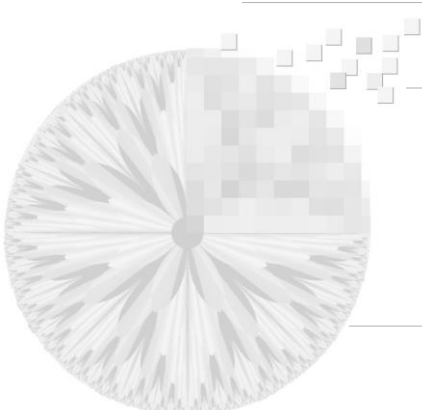


FIGURE 4.18 (a) Original image. (b)–(f) Results of filtering with Gaussian lowpass filters with cutoff frequencies set at radii values of 5, 15, 30, 80, and 230, as shown in Fig. 4.11(b). Compare with Figs. 4.12 and 4.15.

a
b
c
d
e
f



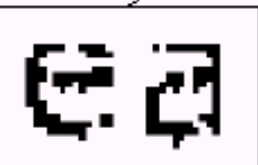
More Examples

a b

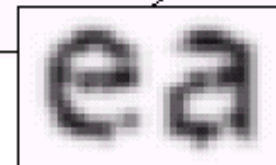
FIGURE 4.19

- (a) Sample text of poor resolution (note broken characters in magnified view).
(b) Result of filtering with a GLPF (broken character segments were joined).

Historically, certain computer programs were written using only two digits rather than four to define the applicable year. Accordingly, the company's software may recognize a date using "00" as 1900 rather than the year 2000.



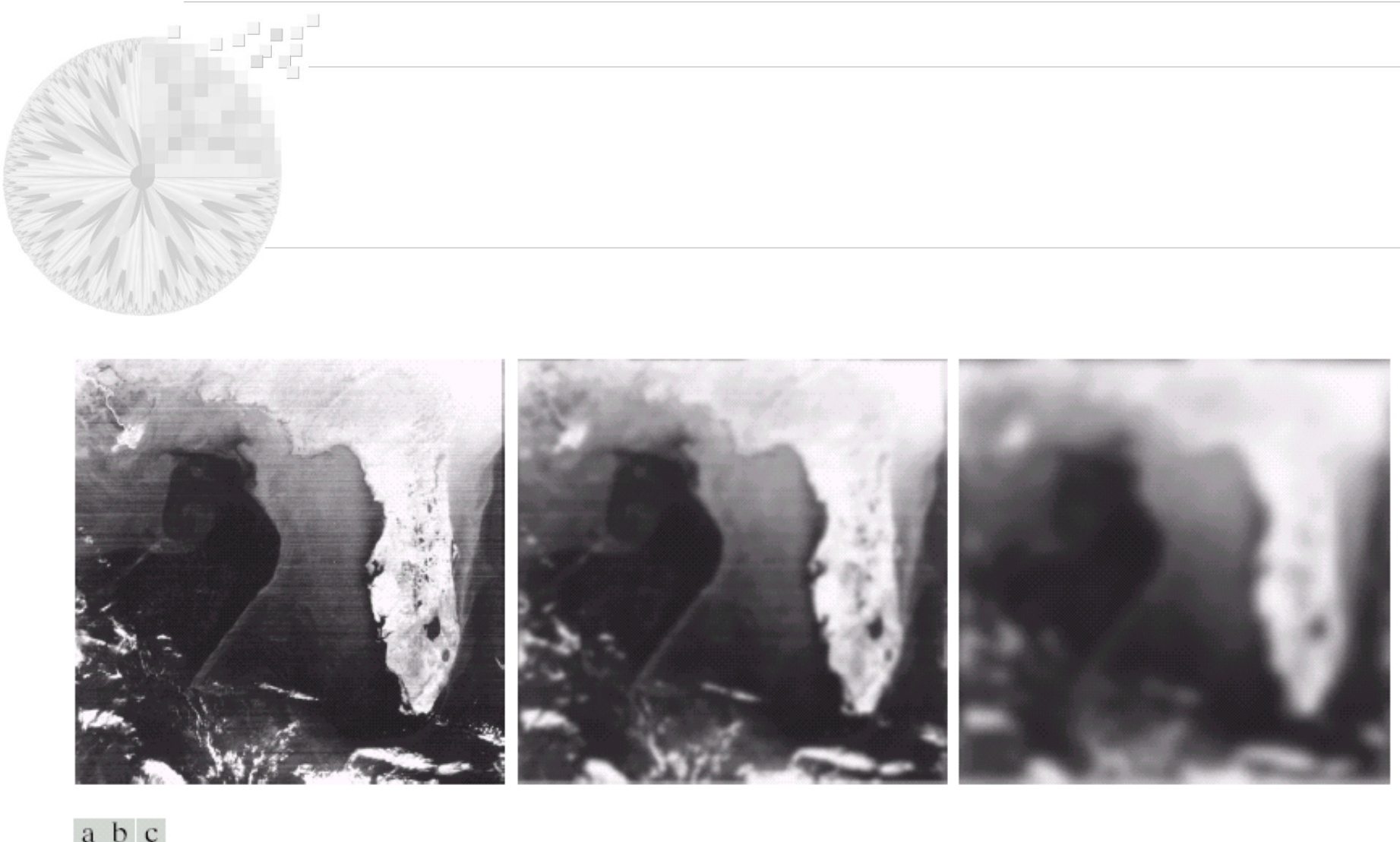
Historically, certain computer programs were written using only two digits rather than four to define the applicable year. Accordingly, the company's software may recognize a date using "00" as 1900 rather than the year 2000.





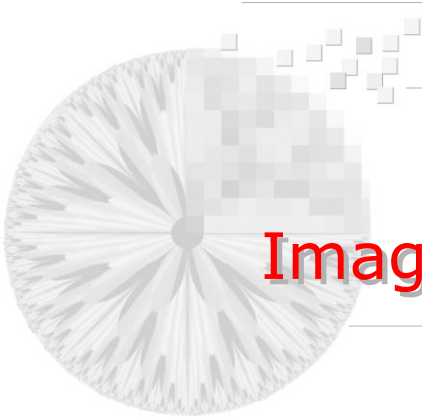
a b c

FIGURE 4.20 (a) Original image (1028×732 pixels). (b) Result of filtering with a GLPF with $D_0 = 100$. (c) Result of filtering with a GLPF with $D_0 = 80$. Note reduction in skin fine lines in the magnified sections of (b) and (c).



a b c

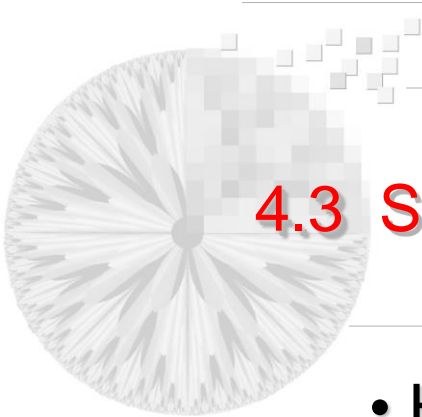
FIGURE 4.21 (a) Image showing prominent scan lines. (b) Result of using a GLPF with $D_0 = 30$. (c) Result of using a GLPF with $D_0 = 10$. (Original image courtesy of NOAA.)



Chapter 4

Image Enhancement in the Frequency Domain

- 4.1 Fundamentals Related to Fourier Transform
- 4.2 Smoothing Using Frequency-Domain Filters
- 4.3 Sharpening Using Frequency-Domain Filters
- 4.4 Implementation

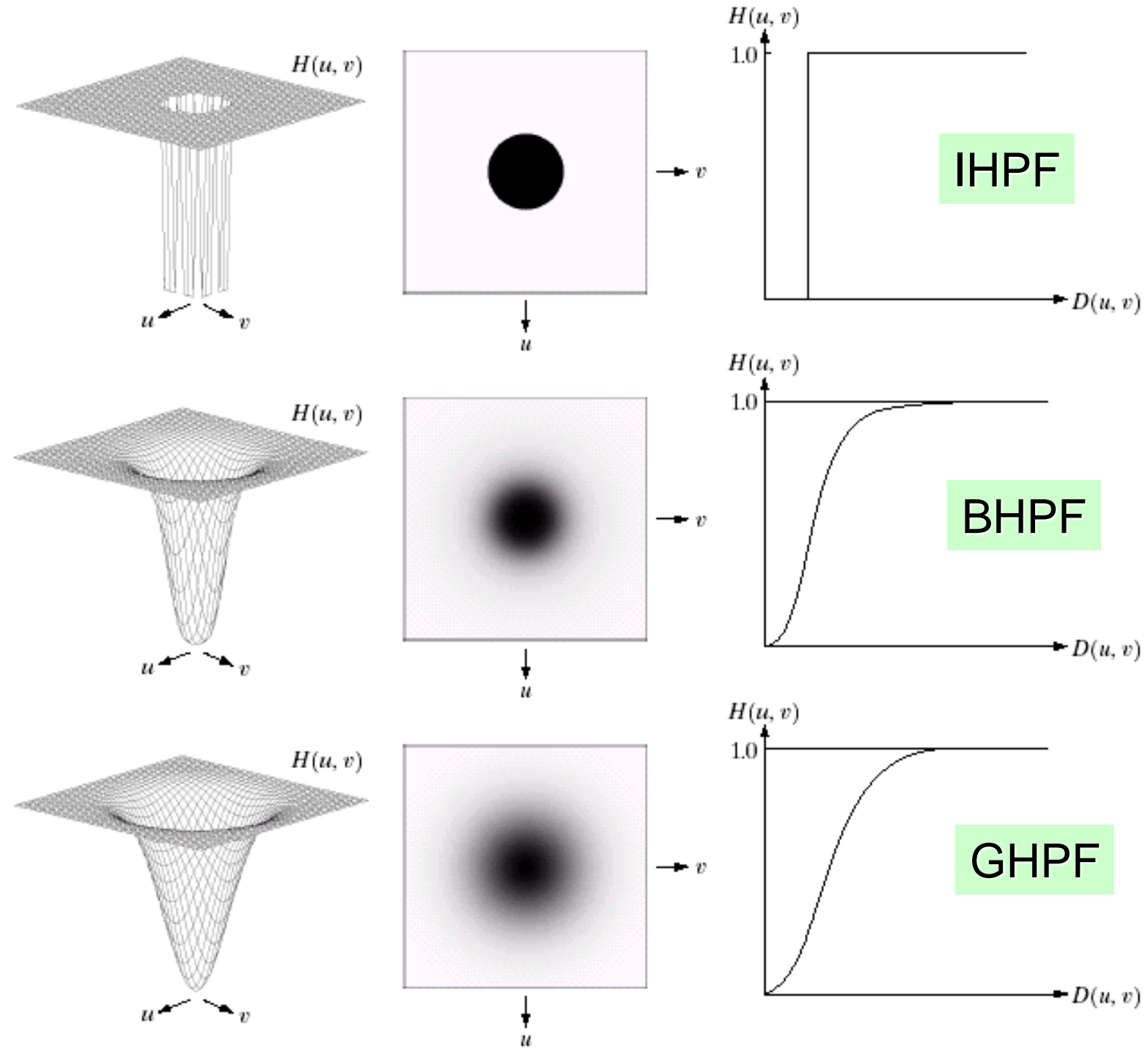


4.3 Sharpening Using Frequency-Domain Filters

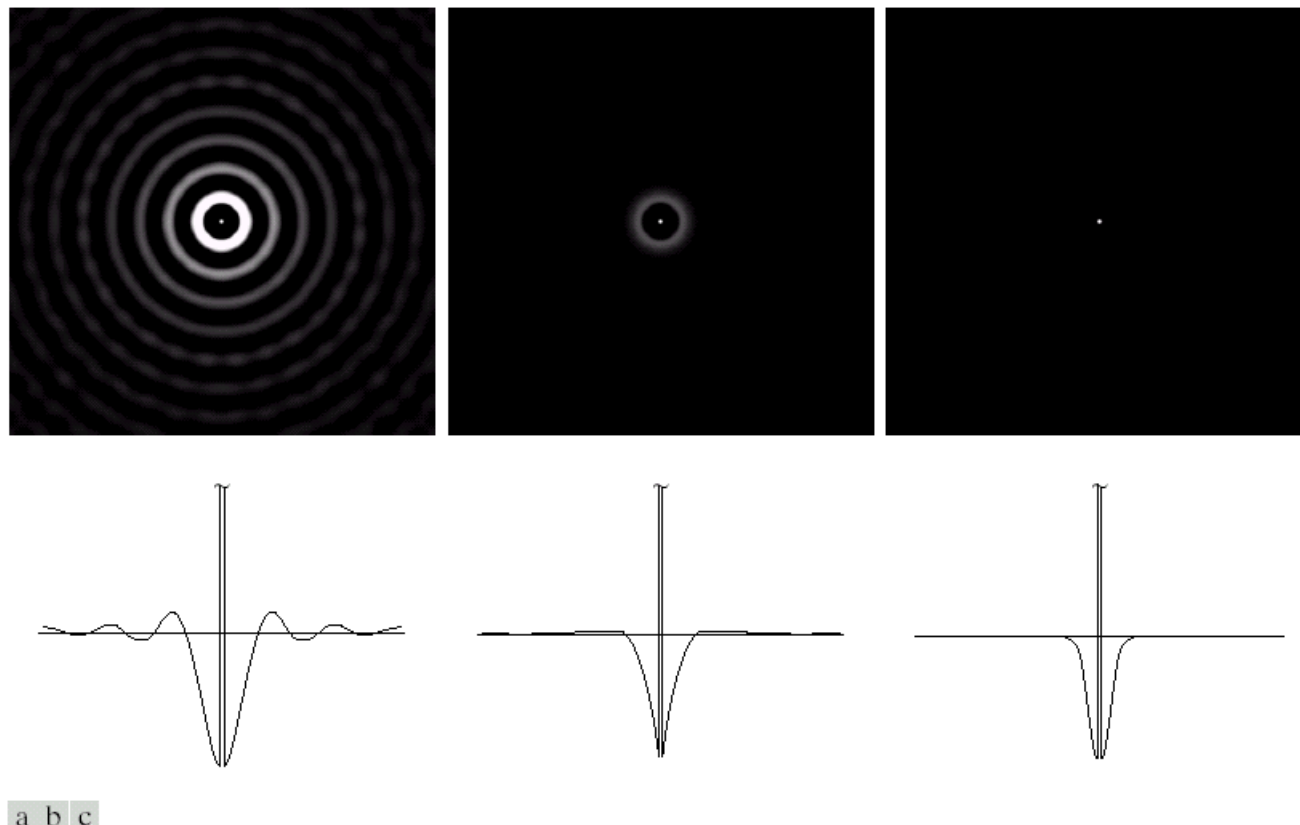
- Highpass Filter, e.g.,

$$H_{hp}(u, v) = 1 - H_{lp}(u, v)$$

- 4.3.1 Ideal Highpass Filters (IHPF)
 - 4.3.2 Butterworth Highpass Filters (BHPF)
 - 4.3.3 Gaussian Highpass Filters (GHPF)
 - 4.3.4 The Laplacian in the Frequency Domain
 - 4.3.5 Homomorphic Filtering

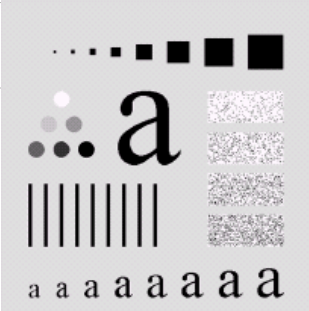
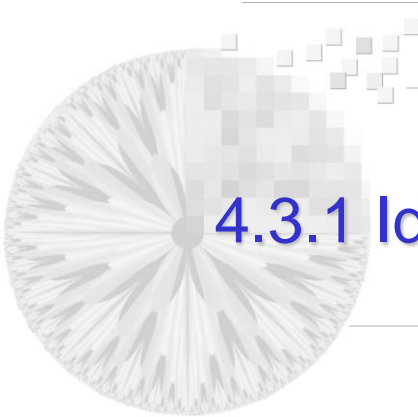


Impulse Responses of IHPF, BHPF, GHPF



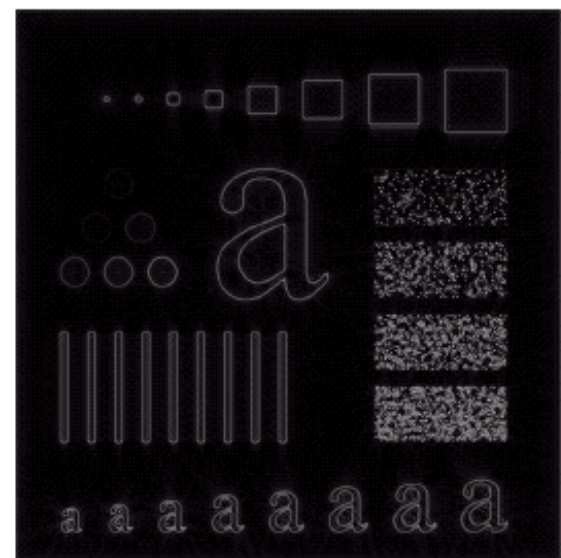
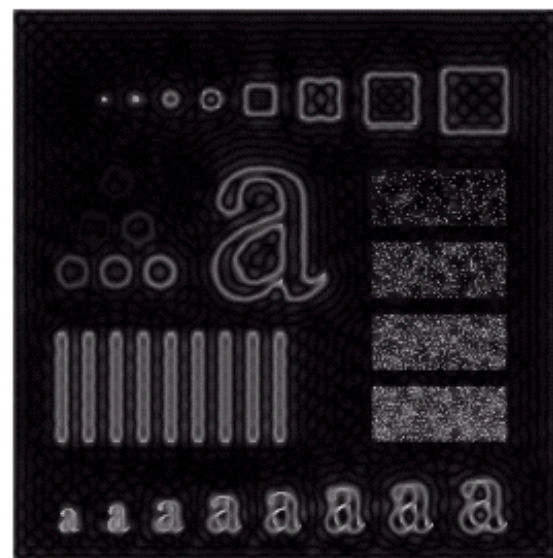
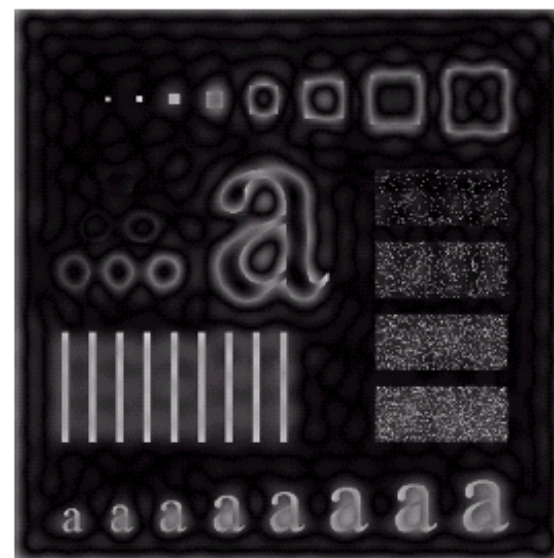
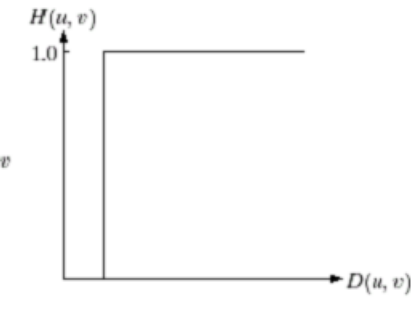
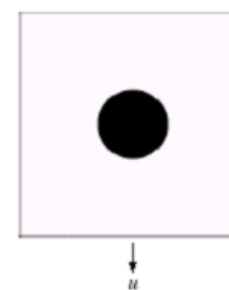
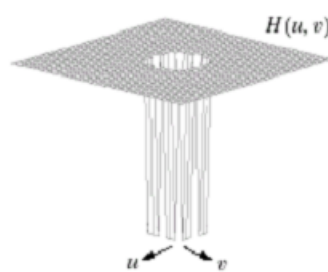
a b c

FIGURE 4.23 Spatial representations of typical (a) ideal, (b) Butterworth, and (c) Gaussian frequency domain highpass filters, and corresponding gray-level profiles.



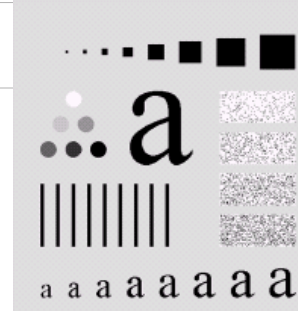
4.3.1 Ideal Highpass Filter

$$H(u, v) = \begin{cases} 0 & \text{if } D(u, v) \leq D_0 \\ 1 & \text{if } D(u, v) > D_0 \end{cases}$$



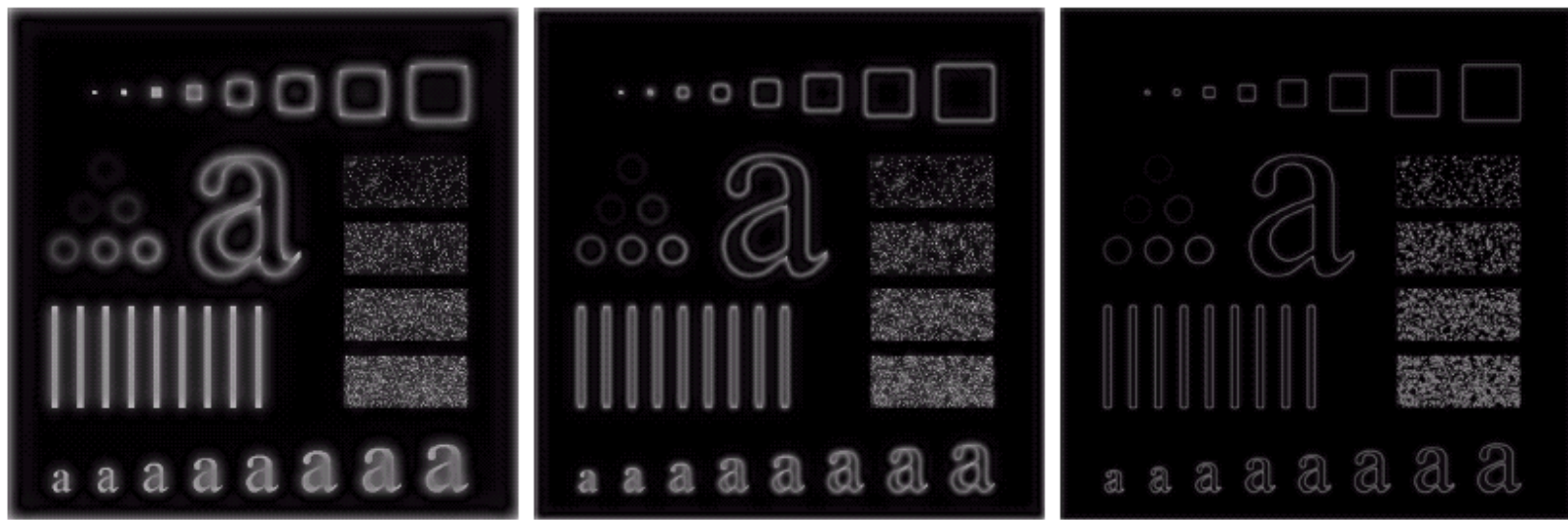
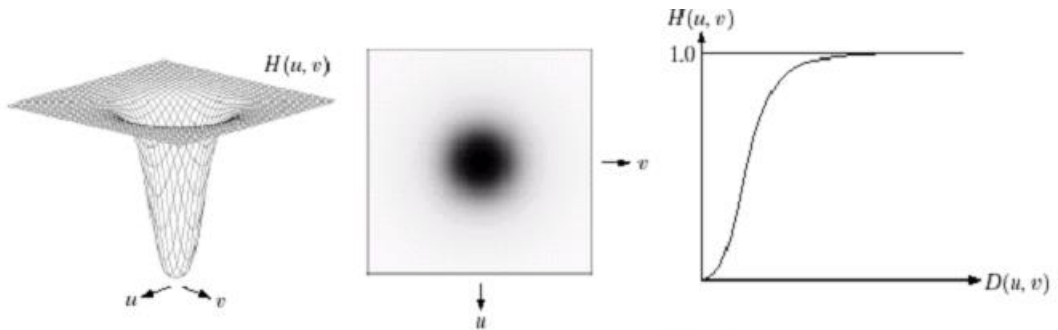
a b c

FIGURE 4.24 Results of ideal highpass filtering the image in Fig. 4.11(a) with $D_0 = 15, 30, and 80 , respectively. Problems with ringing are quite evident in (a) and (b).$



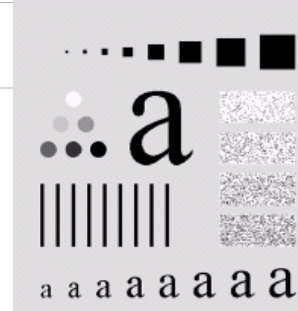
4.3.2 Butterworth Highpass Filter

$$H(u, v) = \frac{1}{1 + [D_0/D(u, v)]^{2n}}$$



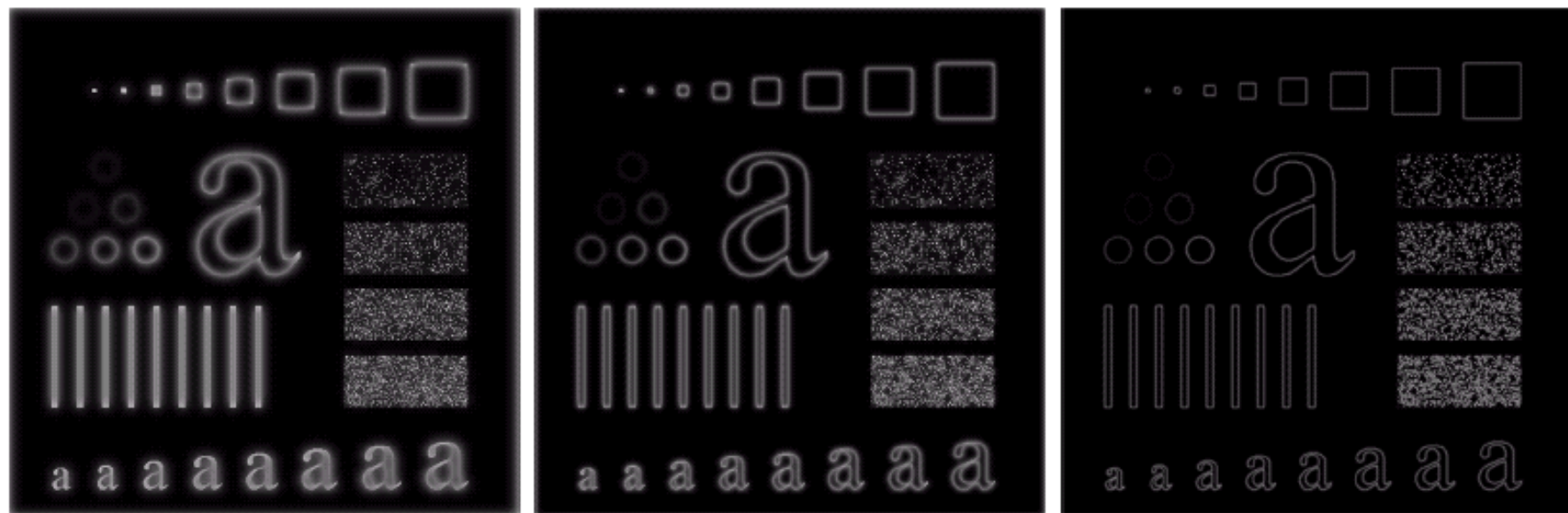
a b c

FIGURE 4.25 Results of highpass filtering the image in Fig. 4.11(a) using a BHPF of order 2 with $D_0 = 15$, 30, and 80, respectively. These results are much smoother than those obtained with an ILPF.



4.3.3 Gaussian Highpass Filter

$$H(u, v) = 1 - e^{-D^2(u, v)/2D_0^2}$$



a b c

FIGURE 4.26 Results of highpass filtering the image of Fig. 4.11(a) using a GHPF of order 2 with $D_0 = 15$, 30, and 80, respectively. Compare with Figs. 4.24 and 4.25.

4.3.4 The Laplacian in the Frequency Domain

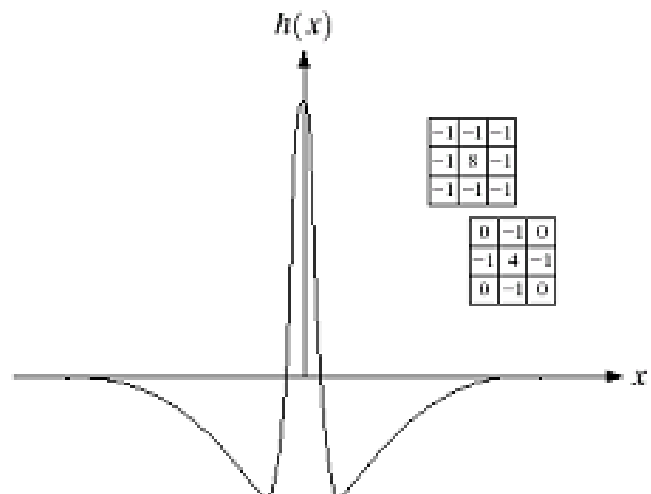
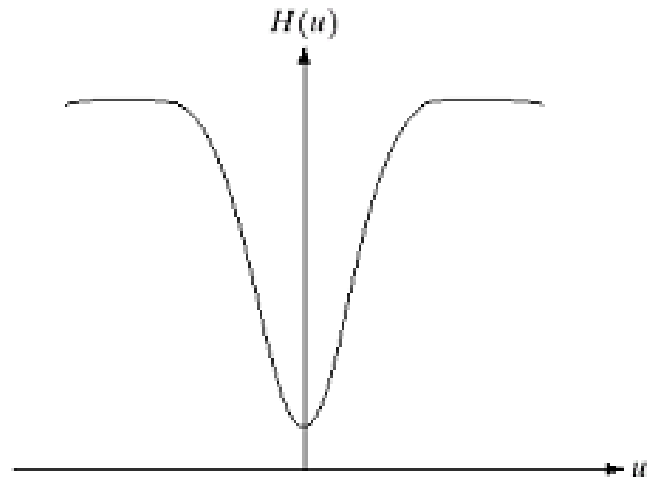
Highpass using a difference of Gaussians
-- more parameters, more control

$$H(u) = Ae^{-u^2/2\sigma_1^2} - Be^{-u^2/2\sigma_2^2}$$

$$h(x) = \sqrt{2\pi}\sigma_1 Ae^{-2\pi^2\sigma_1^2x^2} \\ - \sqrt{2\pi}\sigma_2 Be^{-2\pi^2\sigma_2^2x^2}$$



~ Laplacian in spatial filtering

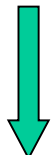


Review 3.7.2 The Laplacian

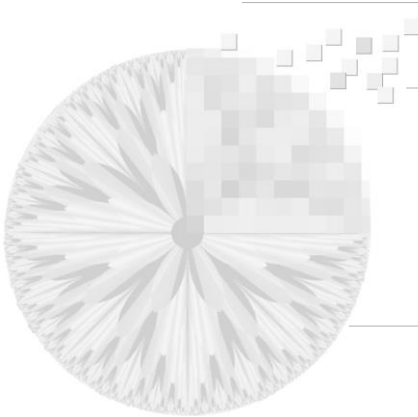
-- isotropic, i.e., rotation-invariant ?

$$\nabla^2 f = \frac{\partial^2 f}{\partial x^2} + \frac{\partial^2 f}{\partial y^2}$$

Discrete form $\left\{ \begin{array}{l} \frac{\partial^2 f}{\partial x^2} = f(x+1, y) + f(x-1, y) - 2f(x, y) \\ \frac{\partial^2 f}{\partial y^2} = f(x, y+1) + f(x, y-1) - 2f(x, y) \end{array} \right.$



$$\nabla^2 f = [f(x+1, y) + f(x-1, y) + f(x, y+1) + f(x, y-1)] - 4f(x, y).$$



Filter Mask for Digital Laplacian

isotropic for increments of 90°

0	1	0
1	-4	1

0	1	0
1	-8	1

0	-1	0
-1	4	-1

1	1	1
1	-8	1

1	1	1
1	1	1

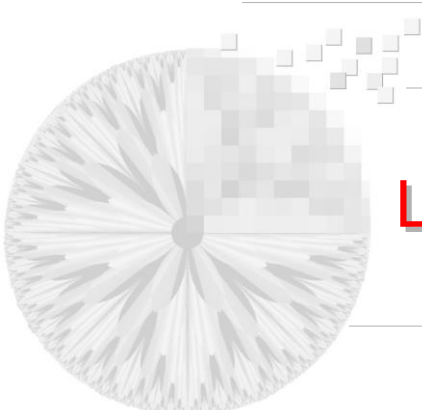
-1	-1	-1
-1	8	-1

including diagonal neighbors
isotropic for increments of 45°

a	b
c	d

FIGURE 3.39

- (a) Filter mask used to implement the digital Laplacian, as defined in Eq. (3.7-4).
(b) Mask used to implement an extension of this equation that includes the diagonal neighbors. (c) and (d) Two other implementations of the Laplacian.



Laplacian-Based Enhancement

$$g(x, y) = \begin{cases} f(x, y) - \nabla^2 f(x, y) & \text{if the center coefficient of the Laplacian mask is negative} \\ f(x, y) + \nabla^2 f(x, y) & \text{if the center coefficient of the Laplacian mask is positive.} \end{cases}$$

$$\begin{aligned} g(x, y) &= f(x, y) - [f(x+1, y) + f(x-1, y) \\ &\quad + f(x, y+1) + f(x, y-1)] + 4f(x, y) \\ &= 5f(x, y) - [f(x+1, y) + f(x-1, y) \\ &\quad + f(x, y+1) + f(x, y-1)]. \end{aligned}$$

An Example of Laplacian-Based Enhancement

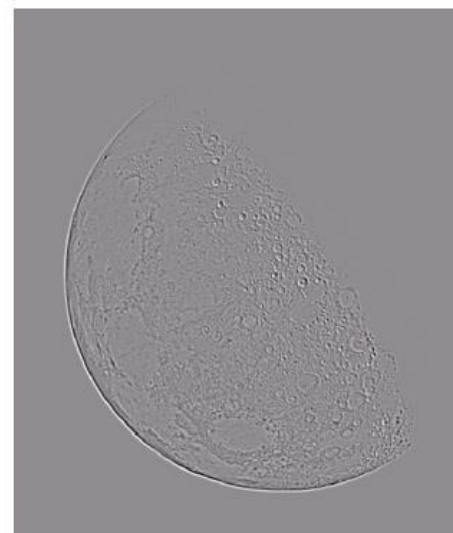
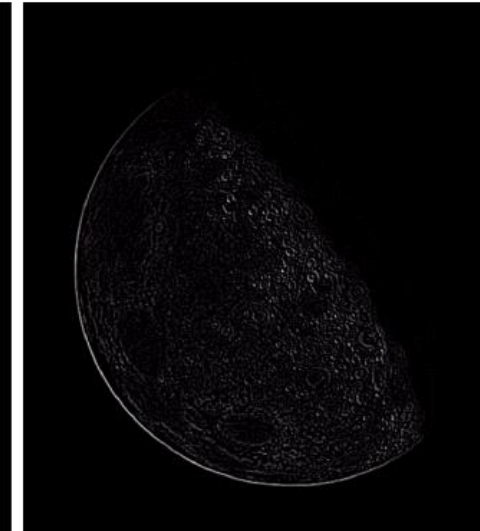
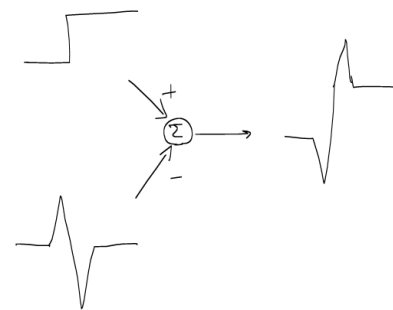
$$\begin{matrix} 0 & 0 & 100 & 100 \\ 0 & 0 & 100 & 100 \\ 0 & 0 & 100 & 100 \end{matrix}$$

a
b
c
d

FIGURE 3.40
(a) Image of the
North Pole of the
moon.

$$\begin{array}{|c|c|c|} \hline 0 & 1 & 0 \\ \hline 1 & -4 & 1 \\ \hline 0 & 1 & 0 \\ \hline \end{array}$$

$$\begin{matrix} 0 & 100 & -100 & 0 \\ 0 & 100 & -100 & 0 \\ 0 & 100 & -100 & 0 \end{matrix}$$



Filter function for the Laplcian operation

$$\Im \left[\frac{d^n f(x)}{dx^n} \right] = (ju)^n F(u)$$

→

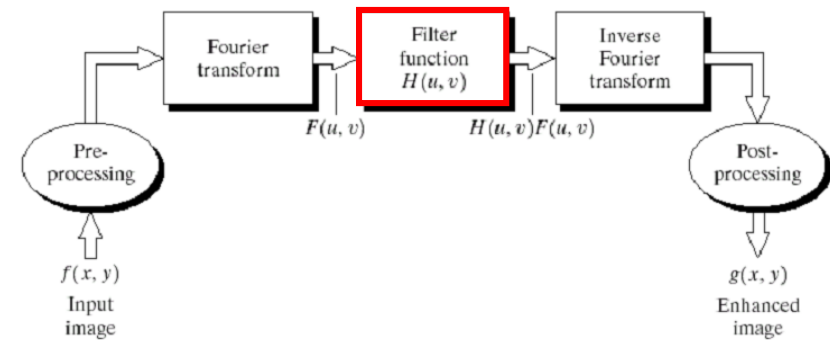
$$\begin{aligned} \Im \left[\frac{\partial^2 f(x, y)}{\partial x^2} + \frac{\partial^2 f(x, y)}{\partial y^2} \right] &= (ju)^2 F(u, v) + (jv)^2 F(u, v) \\ &= -(u^2 + v^2) F(u, v). \end{aligned}$$

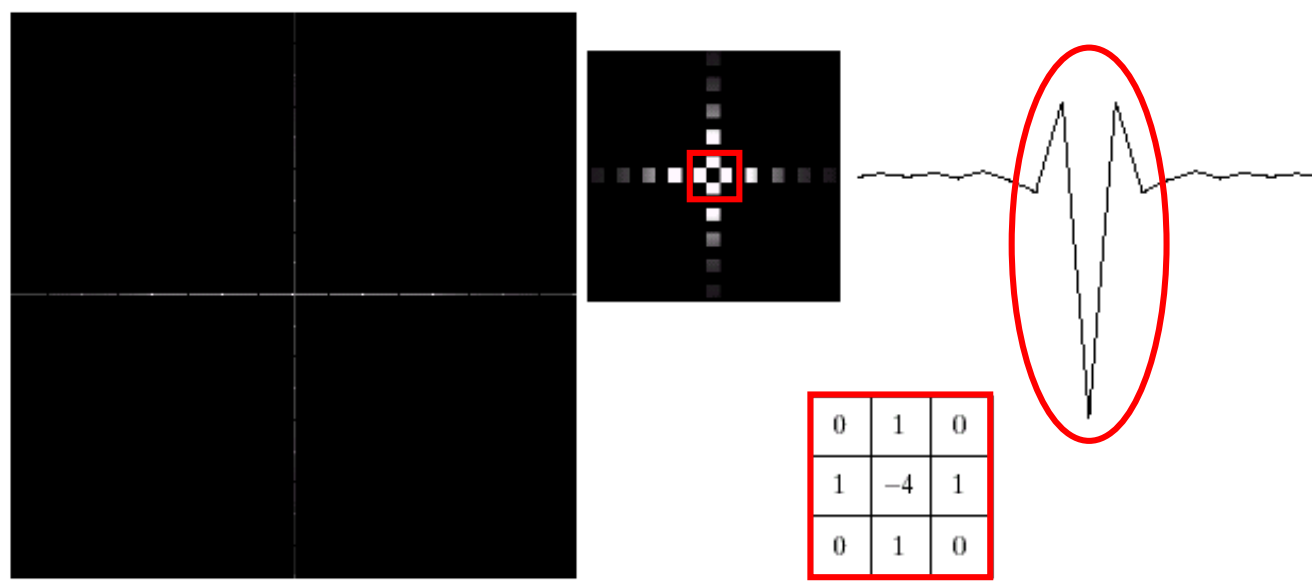
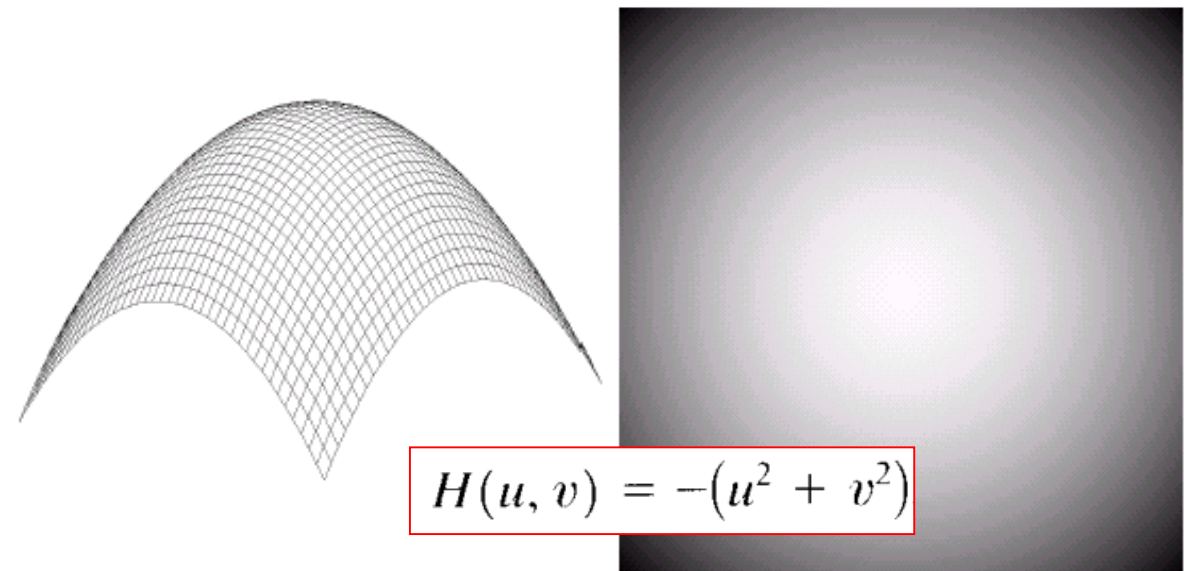
→

$$\Im [\nabla^2 f(x, y)] = -(u^2 + v^2) F(u, v)$$

→

$$H(u, v) = -(u^2 + v^2)$$

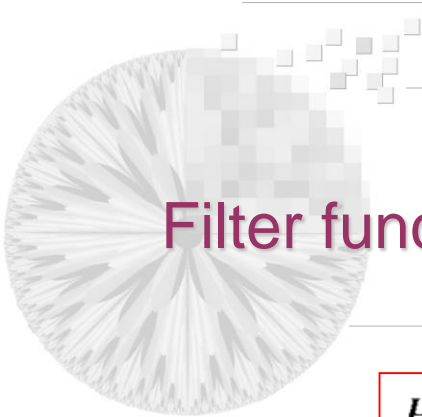




a
b
c
d
e
f

$$\nabla^2 f(x, y) \Leftrightarrow -[(u - M/2)^2 + (v - N/2)^2]F(u, v)$$

FIGURE 4.27 (a) 3-D plot of Laplacian in the frequency domain. (b) Image representation of (a). (c) Laplacian in the spatial domain obtained from the inverse DFT of (b). (d) Zoomed section of the origin of (c). (e) Gray-level profile through the center of (d). (f) Laplacian mask used in Section 3.7.



Filter function for the Laplcian operation

$$H(u, v) = -(u^2 + v^2)$$

Laplacian-Based Enhancement

$$g(x, y) = f(x, y) - \nabla^2 f(x, y)$$

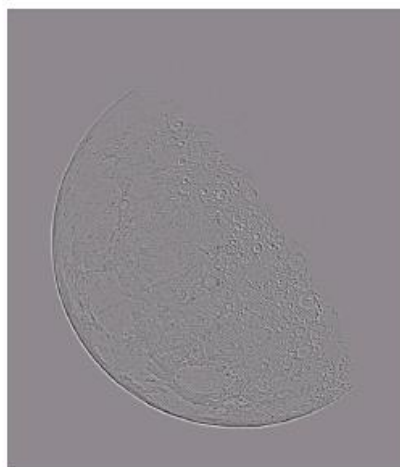
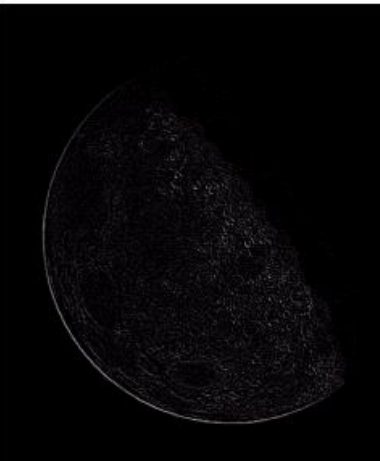
→
$$g(x, y) = \mathfrak{F}^{-1}\{[1 + ((u - M/2)^2 + (v - N/2)^2)]F(u, v)\}$$

Frequency domain vs Spatial domain

a
b
c
d

FIGURE 4.28

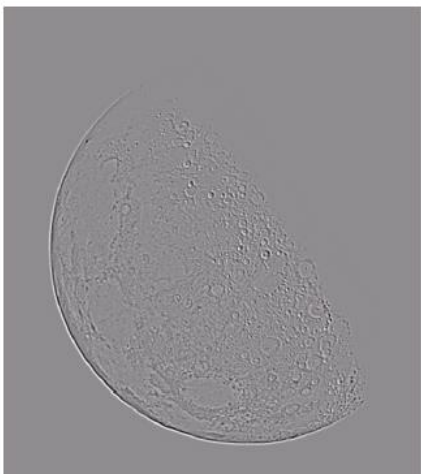
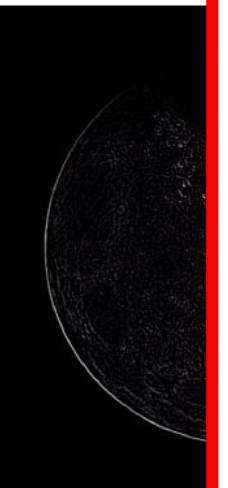
- (a) Image of the North Pole of the moon.
(b) Laplacian filtered image.
(c) Laplacian image scaled.
(d) Image enhanced by using Eq. (4.4-12).
(Original image courtesy of NASA.)



a
b
c
d

FIGURE 3.40

- (a) Image of the North Pole of the moon.
(b) Laplacian-filtered image.
(c) Laplacian image scaled for display purposes.
(d) Image enhanced by using Eq. (3.7-5).
(Original image courtesy of NASA.)



Laplacian-Based Enhancement

4.3.5 Homomorphic Filtering

- Image expressed as the product of illumination and reflectance components:

$$f(x, y) = i(x, y) r(x, y)$$

Illumination: usually varies slowly

$$\Im\{f(x, y)\} \neq \Im\{i(x, y)\} \Im\{r(x, y)\}$$

Reflectance: usually varies abruptly

Define $z(x, y) = \ln f(x, y)$
 $= \ln i(x, y) + \ln r(x, y)$

→ $\Im\{z(x, y)\} = \Im\{\ln f(x, y)\}$
 $= \Im\{\ln i(x, y)\} + \Im\{\ln r(x, y)\}$



$$\begin{aligned}\Im\{z(x, y)\} &= \Im\{\ln f(x, y)\} \\ &= \Im\{\ln i(x, y)\} + \Im\{\ln r(x, y)\}\end{aligned}$$

→ $Z(u, v) = F_i(u, v) + F_r(u, v)$

- Process with a filter $H(u, v)$

→ $\begin{aligned}S(u, v) &= H(u, v)Z(u, v) \\ &= H(u, v)F_i(u, v) + H(u, v)F_r(u, v)\end{aligned}$

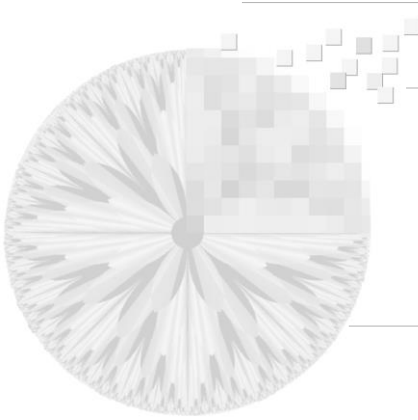
$$S(u, v) = H(u, v)Z(u, v)$$

$$= H(u, v)F_i(u, v) + H(u, v)F_r(u, v)$$

→ $s(x, y) = \mathfrak{I}^{-1}\{S(u, v)\}$
 $= \mathfrak{I}^{-1}\{H(u, v)F_i(u, v)\} + \mathfrak{I}^{-1}\{H(u, v)F_r(u, v)\}.$

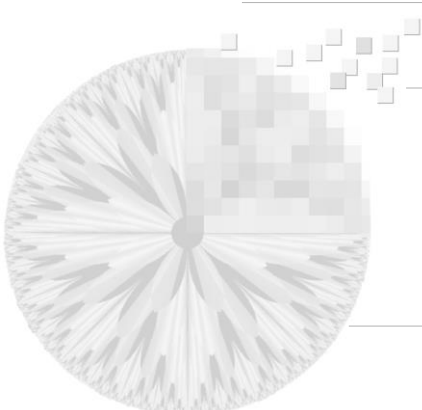
Let $\begin{cases} i'(x, y) = \mathfrak{I}^{-1}\{H(u, v)F_i(u, v)\} \\ r'(x, y) = \mathfrak{I}^{-1}\{H(u, v)F_r(u, v)\} \end{cases}$

→ $s(x, y) = i'(x, y) + r'(x, y)$

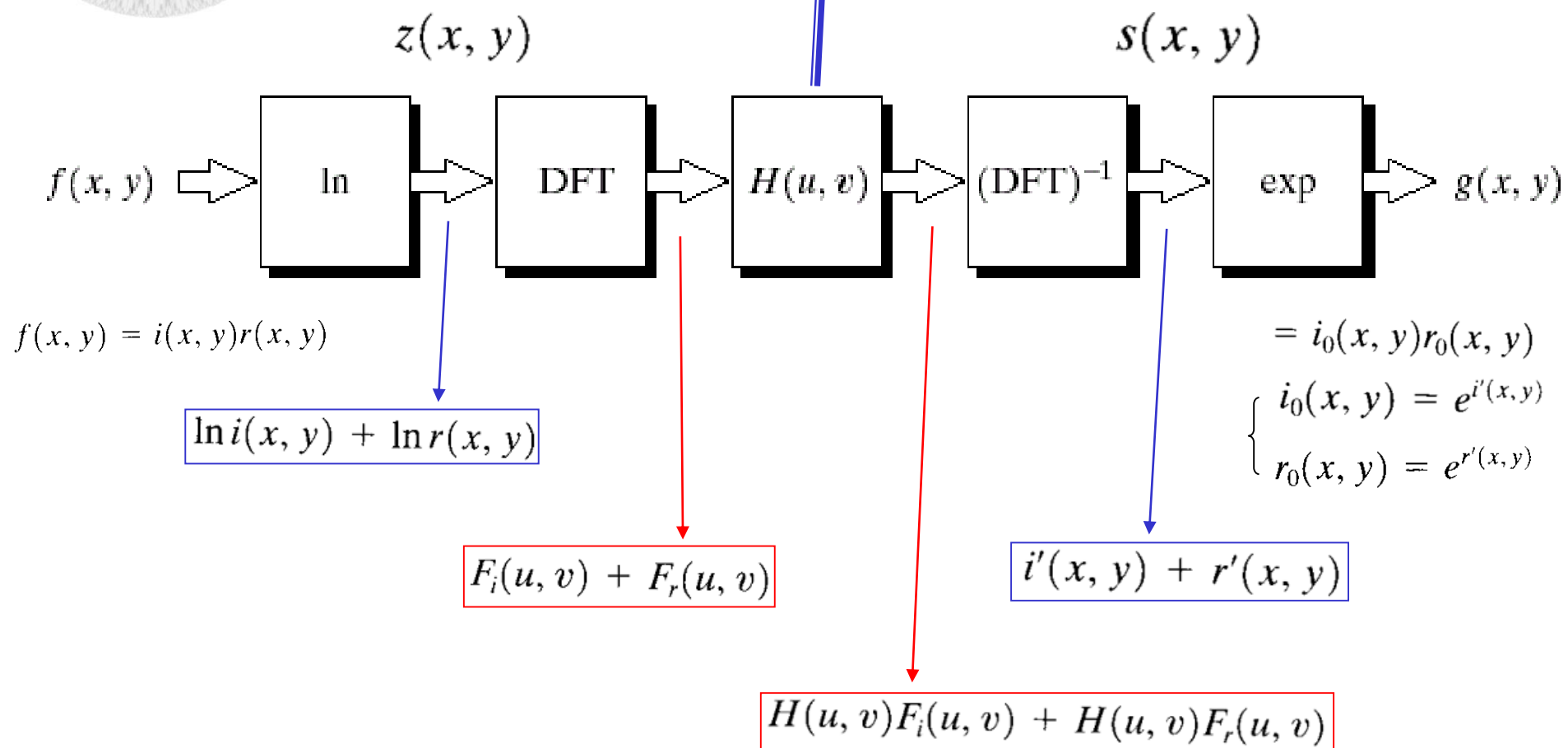


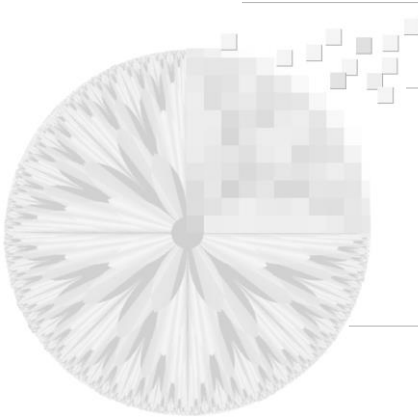
$$\begin{aligned}g(x, y) &= e^{s(x, y)} \\&= e^{i'(x, y)} \cdot e^{r'(x, y)} \\&= i_0(x, y)r_0(x, y)\end{aligned}$$

$$\left\{ \begin{array}{l} i_0(x, y) = e^{i'(x, y)} \\ r_0(x, y) = e^{r'(x, y)} \end{array} \right.$$

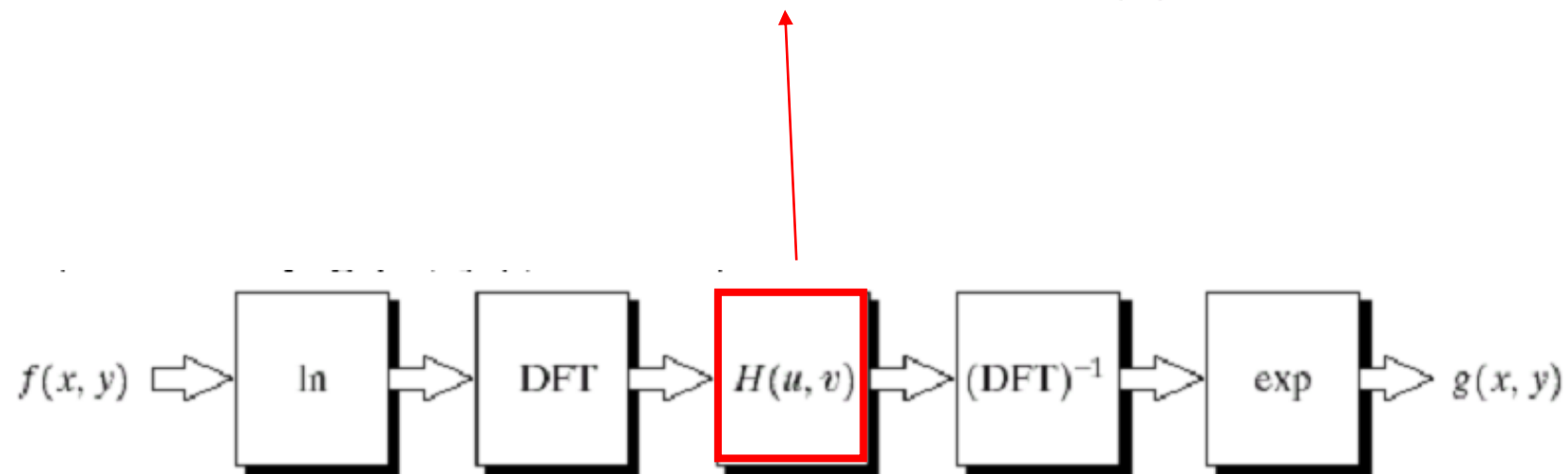
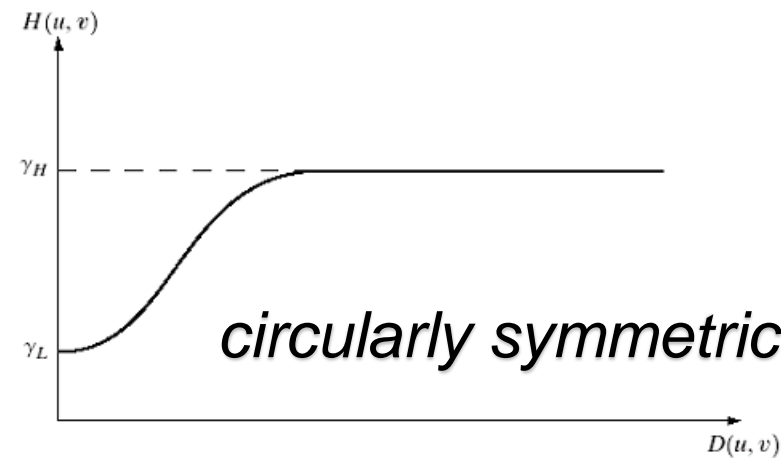


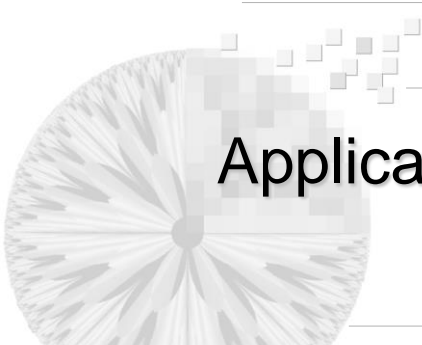
Homomorphic Filter





$$H(u, v) = (\gamma_H - \gamma_L) [1 - e^{-c(D^2(u, v)/D_0^2)}] + \gamma_L$$





Applications: Image Enhancement Display of High Dynamic Range Images



a | b

FIGURE 4.62

(a) Full body PET scan. (b) Image enhanced using homomorphic filtering. (Original image courtesy of Dr. Michael E. Casey, CTI PET Systems.)

